 CMES, vol.91, no.3, pp.153-176, 2013

Iterative Coupling Between the TBEM and the MFS Part I - Acoustic Wave Propagation

António Tadeu[1,2], Julieta António[1], Patrícia Ferreira[3]

Abstract: This paper presents an iterative coupling between a formulation based on the normal derivative of the integral equation (TBEM) and the method of fundamental solutions (MFS) for the transient analysis of acoustic wave propagation problems in the presence of multiple inclusions. The proposed formulation overcomes the individual limitations of each method, requires less computer memory and may use less CPU time than a full direct coupling formulation scheme.
In the proposed formulation each inclusion is solved individually, successively, using the TBEM or the MFS and scatters a field that it is seen as an incident field at each of the other inclusions. The iterative process is stopped when the field scattered by each individual inclusion is negligible. The final solution is the sum of all the scattered field contributions. The inclusions are coupled by imposing the required boundary conditions.
The accuracy of the proposed algorithms, using different numbers of inclusions, is verified by comparing the solutions against reference solutions established by solving a full coupling system. The applicability of the proposed method is shown by simulating the acoustic behavior of a set of rigid acoustic screens in the vicinity of a dome.

Keywords: acoustic wave propagation, iterative TBEM/MFS coupling, thin acoustic barriers

1 Introduction

Solving wave propagation problems in the presence of multiple inclusions of different sizes, types and shapes embedded in unbounded acoustic or elastic media is

[1] Corresponding author. E-mail address: tadeu@itecons.uc.pt Tel. + 351 239 798 921 Fax: + 351 239 798 939
[2] CICC, Department of Civil Engineering, Faculty of Sciences and Technology, University of Coimbra, Rua Luís Reis Santos - Pólo II da Universidade, 3030-788 Coimbra, Portugal
[3] ITeCons, Rua Pedro Hispano and Pólo II da Universidade, 3030-289 Coimbra, Portugal

a challenge for areas of engineering such as acoustics, underwater acoustics, seismology, and electromagnetism. A problem of this nature may give rise to an intricate wave field caused by the interaction between the incident field and multiple reflections between the inclusions.

Analytical approaches are only known for regular geometries such as circular cylindrical cylinders and spheres [Defos du Rau et al. (1996); Huang and Lu (2006); Antoine et al. (2008); Gabrielli and Mercier-Finidori (2001)]. The presence of inclusions of irregular and complex geometries often leads to the implementation of numerical methods such as the boundary element method (BEM), the finite difference method (FDM) or the finite element method (FEM).

The FEM and the FDM are better suited to deal with bounded domains since they require the full discretization of the domain. However, when there are multiple inclusions the space between them also needs to be discretized and special treatments are required. If the domain is unbounded it becomes unfeasible for a very large number of inclusions.

But some advances have been made in simplifying the computation in regions containing complex scatter configurations, such as those applied by Grote and Kirsch (2004). They use several smaller, separate, artificial boundaries, each enclosing a different obstacle. They handle the unboundedness of the physical domain by introducing an extended version of an exact non-reflecting boundary condition known as a Dirichlet-to-Neumann (DtN) condition. The applicability of the DtN technique coupled with finite difference methods is enhanced by extending it to multiple scattering from obstacles of arbitrary shape [Acosta and Villamizar (2010)].

The BEM is one of the most suitable techniques for modeling homogeneous unbounded systems containing irregular interfaces and inclusions since the far field conditions are automatically satisfied and only the boundaries of the interfaces and inclusions need to be discretized. Thus, the numerical errors are attenuated compared with those obtained with full domain discretization methods.

However, the BEM has some drawbacks. The knowledge of appropriate Green's functions is required, which implies the correct evaluation of singular or hypersingular integrals when solving the boundary integral equations and generates complex and fully populated linear systems. Moreover, the classical formulation of the BEM degenerates to lead to ill-conditioned systems in the modeling of thin bodies or open boundary problems (zero thickness structures). In such cases the dual boundary element method or the normal derivative integral equation (named here TBEM) must be used, which causes additional hitches in solving the resulting equations.

The meshfree methods that require neither domain nor boundary discretization have been subjects of recent research in many areas of computational science and approximation theory [Fairweather et al. (2003); Godinho et al. (2009)]. The MFS belongs to the class of boundary methods and it may be seen as an indirect boundary element method [Jawson and Symm (1977)] with a concentrated source instead of a distributed one. Like the boundary element method, it requires the knowledge of fundamental solutions [Greenberg (1971)].

The MFS seems to be particularly effective for studying wave propagation since it overcomes some of the mathematical complexity of the BEM and provides acceptable solutions at substantially lower computational cost [Godinho et al. (2006)]. The MFS solution is computed by using a linear combination of fundamental solutions (Green's functions [Tadeu et al. (2009)]), generated by a set of virtual sources that use a domain decomposition technique to simulate the scattered and refracted field produced by the heterogeneities. To avoid singularities, these fictitious sources are placed at some distance from the inclusion's boundary. The use of fundamental solutions allows the final solution to verify the unbounded boundary conditions automatically. Still, the use of the MFS has its own limitations when thin inclusions such as cracks and inclusions with twisting (sinuous) boundaries are present [Alves and Leitão (2006)]. Coupling different methods to benefit from the advantages of each is one strategy researchers have adopted to improve the results with a view to speeding up analysis and ensuring efficiency, stability, accuracy and flexibility.

Examples of this are the BEM/FEM [Soares and Mansur (2005); Warszawski et al. (2008); He et al. (2011); Rüberg and Schanz (2008); Lie et al. (2001); Zheng et al. (2011)], BEM/ray tracing [Hampel et al. (2008)] or the BEM/MFS [**?**] coupling where each technique is applied to distinct sub-domains.

In previous works the authors coupled the Traction BEM with the MFS to demonstrate the hybrid method's ability to tackle thin fluid-filled inclusions [Tadeu et al. (2010a)], to model the transient analysis of conduction heat transfer in the presence of inclusions [Tadeu et al. (2010b)], to simulate wave propagation in an elastic medium containing elastic, fluid, rigid, and empty heterogeneities, which may be thin [Tadeu and Castro (2011); Castro and Tadeu (2012)].

Even if the flexibility of the model is improved, the conventional (direct) coupling methods require the equations for all subdomains to be assembled into a single, global, equation system. The solution of problems with multiple inclusions, particularly when modeling high excitation frequencies, thus leads to very large systems whose coefficient matrix not banded and not sparse requiring high computational times and high computer memory.

Iterative solvers have been proposed to solve high dimension systems, even when coupling strategies are not used. Examples of this are the works to solve linear systems resulting from BEM formulations. Valente and Pina [Valente and Pina (2001)] explore conjugate gradient type methods as an alternative to the direct solution techniques for three-dimensional problems. The performance of different iterative solvers has been assessed by Marburg and Schneider [Marburg and Schneider (2003)] in acoustic problems to be analyzed by boundary element methods. The generalized minimal residual method has been used by Ylä-Oijala and Järvenpää [Ylä-Oijala and Järvenpää (2006)] to solve the matrix resulting from using a high order boundary element method to solve time harmonic acoustic scattering problems. Alia et al. [Aliaa et al. (2012)] applied a changing minimal residual method based on the Hessenberg process (CMRH) for solving linear systems yielded by the variational boundary element method applied to acoustic problems.

Researchers have proposed a number of iterative methods to avoid having to assemble and solve a global, coupled equation system. Smaller and better conditioned systems of equations can be obtained by analyzing the subdomains separately, where independent discretizations may be considered for each subdomain and suitable solvers can be used for the system of equations of each subdomain. Several works have been published on the time domain analysis of wave propagation problems that makes use of iterative coupling formulations.

A sequential Dirichlet–Neumann method with single relaxation for the iterative coupling of one FEM and BEM domain to be applied to two-dimensional linear elastostatics has been developed by Lin et al. [Lin et al. (1996)] and Feng and Owen [Feng and Owen (1996)]. Soares et al. [Soares et al. (2004)] modified this algorithm to a sequential Neumann–Dirichlet method with single relaxation and extended it for use in 2D transient electrodynamics problems. More recently, Estorff and Hagen [von Estorff and Hagen (2006)] extended this algorithm to obtain a sequential Neumann–Dirichlet method to solve FEM and BEM subdomains in 3D transient elastodynamic analyses. This method has also been applied to other problems such as analysis of fluid-soil-structure interaction [Soares and Mansur (2006)] and acoustic modeling [Soares (2009)].

Other works developed in the frequency domain have made use of iterative methods. Some of them are not related to the coupling technique [Farhat et al. (2000)]. Farhat et al. [Farhat et al. (2000)] presented two two-level domain decomposition (DD) methods for solving iteratively large-scale systems of equations arising from the finite element discretization of high-frequency exterior Helmholtz problems. The first method employs a single Lagrange multiplier field to glue the local solutions at the subdomain interface boundaries. The second method used two Lagrange multiplier fields for the same purpose.

Benamou and Desprès [Benamou and Desprès (1997)] used the domain decomposition method in conjunction with the PML technique as a coupling iterative technique. The domain is split into smaller sub-domains and a sequence of similar sub-problems is solved. The boundary conditions are adjusted iteratively by ad hoc transmission conditions between adjacent sub-domains.

Soares et al. [Soares et al. (2012)] coupled two meshless methods, the method of fundamental solutions (MFS) and the Kansa's method (KM) to model acoustic wave propagation in heterogeneous media. The MFS is employed to simulate the infinite part of the fluid domain and the KM is applied to discretize the heterogeneities of the model. The KM–MFS coupling requires a successive renewal of the variables at the common interfaces (iterative procedure). A relaxation parameter is introduced to ensure and/or to speed up convergence.

In the present work the transient analysis of acoustic wave propagation problems in the presence of multi-inclusions is undertaken by coupling the TBEM and the MFS. The problem is solved iteratively. The TBEM is implemented to model the thin inclusions, while the MFS is used to solve the inclusions whose geometry is regular. At each step, only one inclusion is individually solved, that leads to small system of equations and thus to reduced matrix storage requirements. During the first iteration, each inclusion is solved using its prescribed boundary conditions. The rest of the inclusions are not taken into account; only the incident field and the scattered field generated by the other inclusions (previously modeled) are considered. After the first iteration, each inclusion is subjected to the new scattered field generated by the other inclusions, and this acts as the incident field, which has not yet been taken into account. As the coefficient matrixes remain the same, the systems of equations are only solved once during the first iteration. The iterative process is stopped when the new scattered field elicited by each inclusion is small. This is accomplished by defining a convergence criterion that can be established by following, at each iteration, the computed response to a set of referenced receivers. To illustrate the applicability of the proposed formulation, acoustic physical systems with different numbers of inclusions are solved and the results and the CPU time required are compared with those obtained using a full coupling technique.

The iterative coupling formulation that is applied to multiple inclusions embedded in an unbounded acoustic medium is described in the next section. The iterative coupling formulation is verified against solutions obtained using a full BEM/MFS coupling formulation, which are taken as reference solutions. The number of iterations and the CPU time taken to compute the numerical responses when varying numbers of inclusions, subjected to different steady state acoustic sources, are used to evaluate the computational efficiency of the proposed iterative coupling formulation.

Finally, the applicability of the proposed iterative method is demonstrated by means of a numerical example that simulates the propagation of acoustic waves generated by a line pressure source when a set of barriers is placed in the vicinity of a dome. Time signatures are computed to illustrate the main propagation features.

2 Iterative TBEM/MFS coupling formulation

Consider two two-dimensional irregular cylindrical inclusions, one thin rigid acoustic screen and a rigid inclusion, submerged in a spatially uniform fluid medium of density ρ (Figure 1).

This system is subjected to a harmonic point pressure source at O, placed at $\mathbf{x}_s(x_s, y_s)$, which oscillates with a frequency ω, and originates an incident pressure at $\mathbf{x}(x,y)$,

$$p_{inc}(\mathbf{x},\omega) = AH_0(k_\alpha r_1) \tag{1}$$

where the subscript *inc* represents the incident field, $r_1 = \sqrt{(x-x_s)^2 + (y-y_s)^2}$, A the wave amplitude, $k_\alpha = \frac{\omega}{\alpha}$, α the pressure wave velocity of the fluid medium, and $H_n(\ldots)$ corresponds to second Hankel functions of order n.

Iteration 0 - Step 1: The incident field only illuminates the thin screen and the second inclusion is assumed to be absent (see Figure 2a)

The pressure (p) at any point $\mathbf{x}$ of the spatial domain can be calculated using the Helmholtz equation,

$$\nabla^2 p(\mathbf{x},\omega) + (k_\alpha)^2 p(\mathbf{x},\omega) = 0 \tag{2}$$

As the barrier is thin, the classical boundary element method degenerates. The use of the normal derivative integral equation is one way to overcome this limitation. The normal derivative integral equation can be derived by applying the gradient operator to the boundary integral equation,

$$c\, p^{(0)}(\mathbf{x},\omega) \;=\; -\int_{S_1} H(\mathbf{x},\mathbf{n}_{n1},\mathbf{x}_0,\omega)\, p^{(0)}(\mathbf{x},\omega)\, ds + p_{inc}(\mathbf{x}_0,\mathbf{x}_s,\omega) \tag{3}$$

In these equations, $\mathbf{n}_{n1}$ is the unit outward normal along the boundary of the inclusion S_1; H are the fundamental solutions (Green's functions) for the pressure gradient at $\mathbf{x}$ due to a virtual point pressure load at $\mathbf{x}_0$. p_{inc} is the pressure incident field at x_0, when the point pressure source is located at $\mathbf{x}_s$. The factor c is a constant defined by the shape of the boundary, taking the value $1/2$ if $\mathbf{x}_0 \in S_1$ and S_1 is smooth. The superscript used in $p^{(iter)}$ indicates the number of the iteration.

The Green's functions for pressure gradients in an unbounded medium, in Cartesian coordinates, can be given by:

$$H(\mathbf{x},\mathbf{n}_{n1},\mathbf{x}_0,\omega) = \frac{\mathrm{i}}{4} k_\alpha H_1(k_\alpha\, r)\, \frac{\partial r}{\partial \mathbf{n}_{n1}} \tag{4}$$

with $r=\sqrt{(x-x_0)^2+(y-y_0)^2}$.

The application of the gradient operator to equation (3), which can be seen as assuming the existence of dipole pressure sources (dynamic doublets), leads to

$$a\,p^{(0)}(\mathbf{x}_0,\omega)=-\int_{S_1}\overline{H}(\mathbf{x},\mathbf{n}_{n1},\mathbf{n}_{n2},\mathbf{x}_0,\omega)\,p^{(0)}(\mathbf{x},\omega)\,ds+\overline{p}_{inc}(\mathbf{x}_0,\mathbf{n}_{n2},\mathbf{x}_s,\omega) \tag{5}$$

The Green's functions $\overline{H}$ are defined by applying the traction operator to H, which can be seen as the derivatives of these former Green's functions, to obtain pressure gradients. In these equations, $\mathbf{n}_{n2}$ is the unit outward normal to the boundary S_1 at the collocation points $\mathbf{x}_0$. In this equation, the factor a is null for piecewise planar boundary elements.

The required two-dimensional Green's functions for an unbounded space are now defined as:

$$\begin{aligned}&\bar{H}\left(\mathbf{x},\mathbf{n}_{n1},\mathbf{n}_{n2},\mathbf{x}_0,\omega\right)=\\&\frac{\mathrm{i}}{4}k_\alpha\left\{-k_\alpha H_2\left(k_\alpha\,r\right)\left[\left(\frac{\partial r}{\partial\mathbf{x}}\right)^2\frac{\partial\mathbf{x}}{\partial\mathbf{n}_{n1}}+\frac{\partial r}{\partial\mathbf{x}}\frac{\partial r}{\partial y}\frac{\partial y}{\partial\mathbf{n}_{n1}}\right]+\frac{H_1\left(k_\alpha\,r\right)}{r}\left[\frac{\partial\mathbf{x}}{\partial\mathbf{n}_{n1}}\right]\right\}\frac{\partial\mathbf{x}}{\partial\mathbf{n}_{n2}}+\\&\frac{\mathrm{i}}{4}k_\alpha\left\{-k_\alpha H_2\left(k_\alpha\,r\right)\left[\frac{\partial r}{\partial\mathbf{x}}\frac{\partial r}{\partial y}\frac{\partial\mathbf{x}}{\partial\mathbf{n}_{n1}}+\left(\frac{\partial r}{\partial y}\right)^2\frac{\partial y}{\partial\mathbf{n}_{n1}}\right]+\frac{H_1\left(k_\alpha\,r\right)}{r}\left[\frac{\partial y}{\partial\mathbf{n}_{n1}}\right]\right\}\frac{\partial y}{\partial\mathbf{n}_{n2}}\end{aligned} \tag{6}$$

In Equation (5) the incident field is computed as

$$\overline{p}_{inc}(\mathbf{x},\mathbf{n}_{n2},\mathbf{x}_s,\omega)=\frac{\mathrm{i}A}{2}k_\alpha H_1\left(k_\alpha r_1\right)\left(\frac{x-x_s}{r_1}\frac{\partial\mathbf{x}}{\partial\mathbf{n}_{n2}}+\frac{y-y_s}{r_1}\frac{\partial y}{\partial\mathbf{n}_{n2}}\right) \tag{7}$$

The solution of equation (5) requires the discretization of the interface S_1 (see Figure 2b). In this analysis the interface is discretized with N straight boundary elements, with one nodal point in the centre of each element. This leads to a system of $[N\times N]$ equations ($\underline{\underline{B}p^{(0)}}=\underline{p}_{inc}^{(0)}$).

$$\left[-\bar{H}^{kl}\right]\left[p^{(0)l}\right]=\left[-\bar{p}_{inc}^{(0)k}\right] \tag{8}$$

where $k,l=1,N$, $\bar{H}^{kl}=\int_{C_l}\bar{H}(\mathbf{x}_l,\mathbf{n}_{n1},\mathbf{n}_{n2},\mathbf{x}_k,\omega)\,dC_l$ and C_l is the length of each boundary element.

The integrations in equation (8) are performed through a Gaussian quadrature scheme when the element being integrated is not the loaded one. When the element being

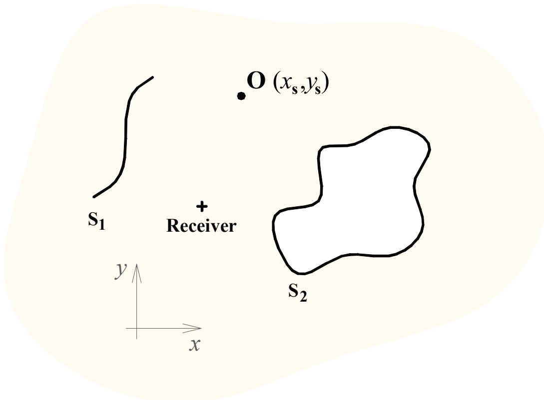

Figure 1: Sketch of the geometry of the problem

integrated (C_l) is the loaded one, the following integral becomes hypersingular,

$$\begin{aligned} &\int_{C_l} \bar{H}\left(\mathbf{x},\mathbf{n}_l,\mathbf{n}_l,\mathbf{x}_0,\omega\right) dC_l = \\ &\int_{C_l} \tfrac{i}{4} k_\alpha \left[-k_\alpha H_2\left(k_\alpha\, r\right) \left(\tfrac{\partial r}{\partial \mathbf{x}} \tfrac{\partial x}{\partial \mathbf{n}_l} + \tfrac{\partial r}{\partial y} \tfrac{\partial y}{\partial \mathbf{n}_l} \right)^2 + \tfrac{H_1(k_\alpha\, r)}{r} \right] dC_l \end{aligned} \tag{9}$$

This integral can be evaluated analytically, considering the dynamic equilibrium of a semi-cylinder bounded by the boundary element, leading to:

$$\int_{C_l} \bar{H}\left(\mathbf{x},\mathbf{n}_l,\mathbf{n}_l,\mathbf{x}_0,\omega\right) dC_l = \frac{i}{2}\left(k_\alpha\right)^2 \left[\int_0^{L/2} H_0\left(k_\alpha\, r\right) dr - \frac{1}{k_\alpha} H_1\left(k_\alpha \frac{L}{2}\right) \right] \tag{10}$$

where L stands for the length of the boundary element. The integral $\int_0^{L/2} H_0\left(k_\alpha\, r\right) dr$ is evaluated, following the expressions in Tadeu *et al.* [Tadeu et al. (1999)]

$$\begin{aligned} \int_0^{L/2} H_0\left(k_\alpha\, r\right) dr = {} & \frac{L}{2} H_0\left(k_\alpha \frac{L}{2}\right) \\ & + \pi \frac{L}{4} \left[H_1\left(k_\alpha \frac{L}{2}\right) S_0\left(k_\alpha \frac{L}{2}\right) - H_0\left(k_\alpha \frac{L}{2}\right) S_1\left(k_\alpha \frac{L}{2}\right) \right] \end{aligned} \tag{11}$$

where $S_{ns}\left(\ldots\right)$ are Struve functions of order ns.

The solution of this system of equations gives the nodal pressures $p^{(0)}$ along the boundary S_1, which allows the scattered pressure field to be defined anywhere in the field $\mathbf{x}_{rec}$,

$$p_{01}(\mathbf{x}_{rec},\omega) = -\int_{S_1} H(\mathbf{x},\mathbf{n}_{n1},\mathbf{x}_{rec},\omega)\, p^{(0)}(\mathbf{x},\omega)\, ds \tag{12}$$

In this equation, the subscripts of $p_{01}(\mathbf{x}_{rec},\omega)$ define the iteration order (0) and identify the structure that produces it (1).

Iteration 0 - Step 2: The rigid inclusion is illuminated by the incident field and by the scattered field generated at the acoustic screen after being submitted to the incident field (Step 1) (see Figure 3a).

The second inclusion, a rigid body, is modeled using the MFS. The MFS assumes that the response of this inclusion is found as a linear combination of fundamental solutions that simulate the pressure field generated by one set of NS virtual sources. These virtual loads are distributed along the inclusion interface at distance δ from that boundary, towards the interior of the inclusion (line $\hat{C}^{(1)}$ in Figure 3b), in order to prevent singularities. Sources inside the inclusion have unknown amplitudes $a^{(iter)}_{n\_ext}$ (the superscript $(iter)$ indicates the number of the iteration). In the acoustic medium, the scattered pressure fields are given by

$$p^{(0)}(\mathbf{x},\omega) = \sum_{n=1}^{NS}\left[a^{(0)}_{n\_ext} G(\mathbf{x},\mathbf{x}_{n\_ext},\omega)\right] \tag{13}$$

where $G(\mathbf{x},\mathbf{x}_{n\_ext},\omega)$ are the fundamental solutions which represent the pressures at points $\mathbf{x}$, generated by pressure loads acting at positions $\mathbf{x}_{n\_ext}$. $\mathbf{n}\_ext$ are the subscripts that denote the load order number placed along the line $\hat{C}^{(1)}$.

To determine the amplitudes of the unknown virtual pressure loads $a^{(iter)}_{n\_ext}$, null normal pressure gradients must be imposed at interface S_2, along NS collocation points $\mathbf{x}_{col}$. This must be done taking into account the scattered field generated at inclusion 1, the rigid screen. The pressure gradient field generated by the first inclusion defined in *Step 1*, can be viewed as an incident field that strikes the rigid inclusion

$$\frac{\partial p^{(0)}_{12}}{\partial \mathbf{n}_{n2}}(\mathbf{x}_{col},\mathbf{n}_{n2},\omega) = -\int_{S_1} \frac{\partial H}{\partial n_{n2}}(\mathbf{x},\mathbf{n}_{n1},\mathbf{n}_{n2},\mathbf{x}_{col},\omega)\, p^{(0)}(\mathbf{x},\omega)\, ds,$$

$$\frac{\partial p^{(0)}_{12}}{\partial \mathbf{n}_{n2}}(\mathbf{x}_{col},\mathbf{n}_{n2},\omega) + \frac{\partial p_{inc}}{\partial \mathbf{n}_{n2}}(\mathbf{x}_{col},\mathbf{n}_{n2},\mathbf{x}_s,\omega) + \sum_{n=1}^{NS}\left[a^{(0)}_{n\_ext}\frac{\partial G}{\partial \mathbf{n}_{n2}}(\mathbf{x}_{col},\mathbf{n}_{n2},\mathbf{x}_{n\_ext},\omega)\right] = 0 \tag{14}$$

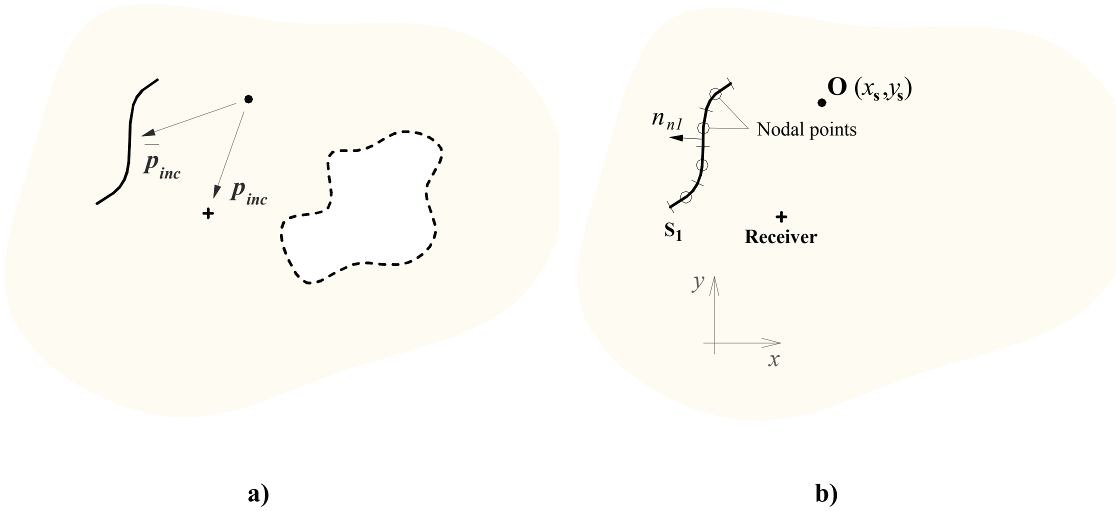

Figure 2: Iteration 0, step 1: a) geometry of the problem; b) discretization of the rigid acoustic screen: nodal points and boundary elements

In these equations, $\mathbf{n}_{n2}$ is the unit outward normal to the boundary S_2.

This leads to a system of $[NS \times NS]$ equations ($\underline{\underline{C}}a^{(0)} = \frac{\partial p_{inc}^{(0)}}{\partial \mathbf{n}_{n2}}$), which allows the unknown amplitudes $a_{n\_ext}^{(0)}$ to be defined.

$$\left[\frac{\partial G_p^{nn}}{\partial \mathbf{n}_{n2}}\right]\left[a_{n\_ext}^{(0)}\right] = \left[-\frac{\partial p_{inc}^{(0)}}{\partial \mathbf{n}_{n2}}\right] \tag{15}$$

where $n = 1, NS$, $\frac{\partial p_{inc}^{(0)}}{\partial \mathbf{n}_{n2}}(\mathbf{x}_{col}, \mathbf{n}_{n2}, \omega) = \frac{\partial p_{12}^{(0)}}{\partial \mathbf{n}_{n2}}(\mathbf{x}_{col}, \mathbf{n}_{n2}, \omega) + \frac{\partial p_{inc}}{\partial \mathbf{n}_{n2}}(\mathbf{x}_{col}, \mathbf{n}_{n2}, \mathbf{x}_s, \omega)$. The scattered field at $\mathbf{x}_{rec}$can then be obtained as

$$p_{02}(\mathbf{x}_{rec}, \omega) = \sum_{n=1}^{NS}\left[a_{n\_ext}^{(0)} G(\mathbf{x}_{rec}, \mathbf{x}_{n\_ext}, \omega)\right] \tag{16}$$

At the end of this iteration the total pressure at the receiver would be

$$p(\mathbf{x}_{rec}, \omega) = p_{inc}(\mathbf{x}_{rec}, \mathbf{x}_s, \omega) + \sum_{m=1}^{M} p_{0\,m}(\mathbf{x}_{rec}, \omega) \tag{17}$$

In this case $M = 2$ (the number of inclusions).

Iteration k - Step 1: The first inclusion is only illuminated by the field scattered by the second inclusion in the conditions defined in the iteration k-1 at Step 2 (see Figure 4a).

At this step the incident field is the scattered field generated by the second inclusion in the previous iteration

$$\overline{p}_{21}^{(k-1)}(\mathbf{x}_0, \mathbf{n}_{n2}, \mathbf{x}_{n\_ext}, \omega) = \sum_{n=1}^{NS} \left[a_{n\_ext}^{(k-1)} \bar{G}(\mathbf{x}_0, \mathbf{n}_{n2}, \mathbf{x}_{n\_ext}, \omega) \right] \tag{18}$$

which leads to

$$a\, p^{(k)}(\mathbf{x}_0, \omega) = -\int_{S_1} \overline{H}(\mathbf{x}, \mathbf{n}_{n1}, \mathbf{n}_{n2}, \mathbf{x}_0, \omega)\, p^{(k)}(\mathbf{x}, \omega)\, ds + \overline{p}_{21}^{(k-1)}(\mathbf{x}_0, \mathbf{n}_{n2}, \mathbf{x}_{n\_ext}, \omega) \tag{19}$$

The solution of this equation leads to a system of $[N \times N]$ equations, similar to the previous one, where only the constant matrix needs to be modified ($\underline{\underline{B}}\underline{p}^{(k)} = \underline{\bar{p}}_{inc}^{(k)}$). Thus, if during iteration 0 the system has been solved by defining its inverse matrix $\underline{\underline{B}}^{-1}$, the new solution does not require the system to be solved, $\underline{p}^{(k)} = \underline{\underline{B}}^{-1}\underline{\bar{p}}_{inc}^{(k)}$. The scattered pressure field at receiver $\mathbf{x}_{rec}$ can then be computed as

$$p_{k1}(\mathbf{x}_{rec}, \omega) = -\int_{S_1} H(\mathbf{x}, \mathbf{n}_{n1}, \mathbf{x}_{rec}, \omega)\, p^{(k)}(\mathbf{x}, \omega)\, ds \tag{20}$$

Iteration k - Step 2: The second inclusion is now only illuminated by the field scattered by the first inclusion at Step 1 (see Figure 4b).

The pressure gradient field generated by the first inclusion at the *Step 1*, is seen as the only incident field that strikes the rigid inclusion

$$\frac{\partial p_{12}^{(k)}}{\partial \mathbf{n}_{n2}}(\mathbf{x}_{col}, \mathbf{n}_{n2}, \omega) = -\int_{S_1} \frac{\partial H}{\partial \mathbf{n}_{n2}}(\mathbf{x}, \mathbf{n}_{n1}, \mathbf{n}_{n2}, \mathbf{x}_{col}, \omega)\, p^{(k)}(\mathbf{x}, \omega)\, ds,$$

which leads to

$$\frac{\partial p_{12}^{(k)}}{\partial \mathbf{n}_{n2}}(\mathbf{x}_{col}, \mathbf{n}_{n2}, \omega) + \sum_{n=1}^{NS} \left[a_{n\_ext}^{(k)} \frac{\partial G}{\partial \mathbf{n}_{n2}}(\mathbf{x}_{col}, \mathbf{n}_{n2}, \mathbf{x}_{n\_ext}, \omega) \right] = 0 \tag{21}$$

This leads to the system of $[NS \times NS]$ equations ($\underline{\underline{C}}\underline{a}^{(k)} = \frac{\partial \underline{p}_{inc}^{(k)}}{\partial \mathbf{n}_{n2}}$), similar to the one defined above in equation (15) where only the constant matrix needs to be replaced

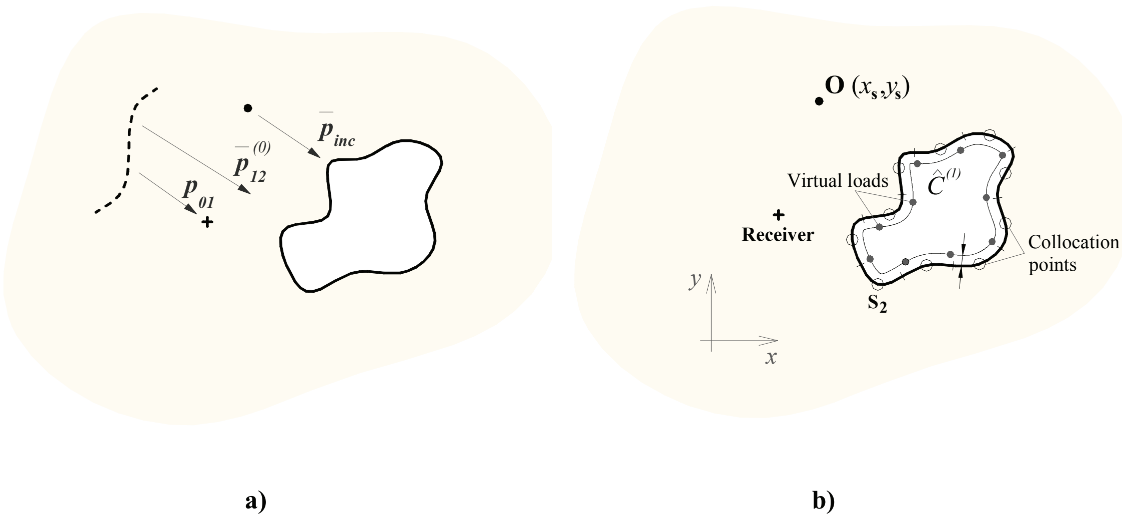

Figure 3: Iteration 0, step 2: a) geometry of the problem; b) rigid inclusion:position of virtual loads and collocation points

by $\frac{\partial p_{inc}^{(k)}}{\partial \mathbf{n}_{n2}}(\mathbf{x}_{col}, \mathbf{n}_{n2}, \omega) = \frac{\partial p_{12}^{(k)}}{\partial \mathbf{n}_{n2}}(\mathbf{x}_{col}, \mathbf{n}_{n2}, \omega)$. The values $a_{n\_ext}^{(k)}$ can thus be obtained as $\underline{a}^{(k)} = \underline{\underline{C}}^{-1} \frac{\partial \underline{p}_{inc}^{(k)}}{\partial \mathbf{n}_{n2}}$.

The new scattered field produced by this inclusion at $\mathbf{x}_{rec}$ is then

$$p_{k2}(\mathbf{x}_{rec}, \omega) = \sum_{n=1}^{NS} \left[a_{n\_ext}^{(k)} G(\mathbf{x}_{rec}, \mathbf{x}_{n\_ext}, \omega) \right] \tag{22}$$

At the end of the iteration k the total pressure at the receiver would be

$$p(\mathbf{x}_{rec}, \omega) = p_{inc}(\mathbf{x}_{rec}, \mathbf{x}_s, \omega) + \sum_{iter=0}^{k} \sum_{m=1}^{M} p_{iter\,m}(\mathbf{x}_{rec}, \omega) \tag{23}$$

The iterative process then continues until the contribution of the last scattered field to the pressure at a certain receiver reaches a predefined threshold.

The proposed iterative coupling requires only the solution of the individual inclusions' linear system of equations. Given the example used to illustrate the algorithm procedure, two individual systems of $[N \times N]$ and $[NS \times NS]$ equations would only be need to be solved once. The full coupling would requires a system of $[(N+NS) \times (N+NS)]$ equations to be solved. This process would more relevant in the presence of a large number of inclusions, when the size of the system of equations used by the full coupling would be very large when compared with the systems associated with each inclusion, as used in the proposed iterative coupling.

3 Pressure in time-space

Given that the computations are performed in the frequency domain, time responses in the space domain are computed by applying an inverse (fast) Fourier transform in ω, using a Ricker pulse as the dynamic excitation source, with temporal variation given by:

$$u(\tau) = D(1-2\tau^2)e^{-\tau^2} \tag{24}$$

where D represents the amplitude; and $\tau = (t - t_s)/t_0$, with t being the time, t_s the time when the wavelet takes its maximum value, and πt_0 the characteristic (dominant) period of the Ricker wavelet.

The application of a Fourier transformation to this function, leads to:

$$U(\omega) = D\left[2t_0\sqrt{\pi}\, e^{-i\omega t_s}\right]\, \Omega^2 e^{-\Omega^2} \tag{25}$$

with $\Omega = \omega t_0/2$.

The Fourier transformation is computed by adding together a finite number of terms. This process corresponds to adding together equally spaced sources with time intervals of $T = 2\pi/\Delta\omega$. In these expressions the frequency increment is defined by $\Delta\omega$. It is essential that $\Delta\omega$ is small enough to avoid contaminating the response in the time domain (aliasing phenomena). This is almost eliminated by the introduction of complex frequencies with a small imaginary part of the form $\omega_c = \omega - i\eta$ (with $\eta = 0.7\Delta\omega$). Note, that $\eta = 0.7\Delta\omega$ will lead to an attenuation of about $\frac{1}{81}$ at the end of the time window given by $\frac{2\pi}{\Delta\omega}$. This procedure is later taken into account by rescaling the responses in the time domain with an exponential factor $e^{\eta t}$ [Kausel and Roesset (1992)].

4 Performance of the proposed iterative coupling formulation

The performance of the proposed iterative coupling formulations is illustrated by computing the acoustic behavior of a set of rigid acoustic screens in the vicinity of a dome, placed in a half-space. Different number of acoustics screens are modeled and subjected to steady state acoustic noise excited by a source emitting different frequencies of excitation.

The CPU times are computed and compared with those given by a full coupling formulation. The responses are calculated assuming a complex frequency with a small imaginary part of the form $\omega_c = \omega - i\eta$ (with $\eta = 0.7\Delta\omega$). $\Delta\omega$ is defined so as to obtain a desired period of simulation $T = 2\pi/\Delta\omega$ in the time domain. Thus, a small $\Delta\omega$ corresponds to lower values of damping and to longer time window.

The wave velocity allowed in the host medium and its density are kept constant at 340 m/s and 1.22 kg/m^3, respectively.

Rigid acoustic screens placed in the vicinity of a dome are used to illustrate the capabilities of the proposed iterative TBEM/MFS formulation. The pressure source is placed at $(3.0, 0.5)$ m, as Figure 5 shows. The barriers, 3.0 m tall, are placed at $x = 10.0$ m (Case 1), $x = 0.0$ m (Case 2) and $x = 12.0$ m (Case 3) in the vicinity of a semi-circular dome with a radius of 7.0 m, centered at $(25.0, 0.0)$ m.

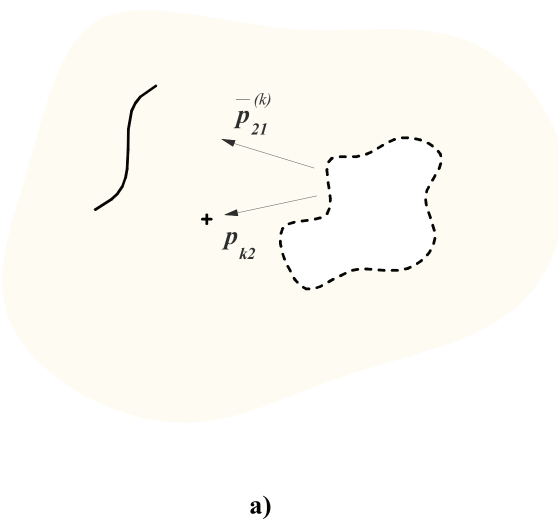

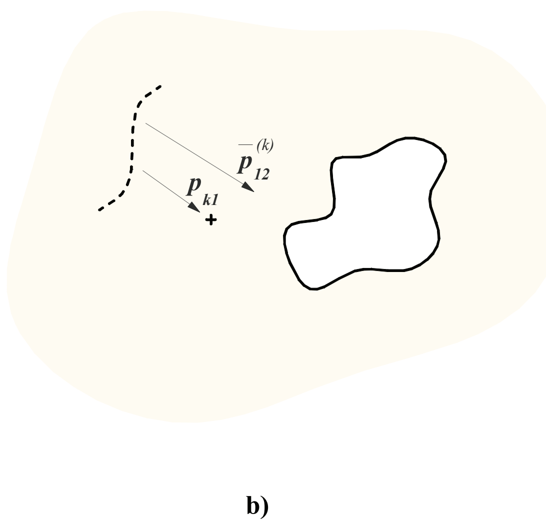

Figure 4: Iteration k: a) step 1; b) step 2

The pressure response is obtained over a two-dimensional grid of 18269 receivers arranged along the x and y directions at equal intervals and placed in the vicinity of the acoustic barriers and dome from $x = -5.0$m to $x = 40.0$m and from $y = 0.0$m to $y = 10.0$m.

Each acoustic barrier is modeled as a rigid screen using the TBEM. It has null-thickness and is discretized using 100 boundary elements. The dome is assumed to be rigid and simulated by the MFS, using 200 virtual loads/collocation points. In the present example, the virtual loads are placed 0.7 m from its boundary. The problem uses Green's functions appropriate for a half-space, assuming a rigid floor.

The real and imaginary responses computed using the full coupling are displayed for each case and the associated CPU time is recorded. For this, the CPU time is computed individually for each grid's receiver. In addition, the number of iterations and the CPU time are registered when each problem is solved using the iterative coupling. The iteration loop is stopped and the number of iterations registered when the pressure at each individual receiver does not change in relation to the prior iteration by more than a predefined threshold that has been set to

$$\left|\sum_{iter=0}^{k}\sum_{m=1}^{M} p_{iter\,m}(\mathbf{x}_{rec},\omega)-\sum_{iter=0}^{k-1}\sum_{m=1}^{M} p_{iter\,m}(\mathbf{x}_{rec},\omega)\right| / \left|\sum_{iter=0}^{k}\sum_{m=1}^{M} p_{iter\,m}(\mathbf{x}_{rec},\omega)\right| \leq 1E-05. \quad (26)$$

Two different excitation frequencies have been selected to illustrate the main findings, $f = 2.0$ Hz and $f = 100.0$ Hz.

Analysis of the responses shows that the number of iterations changes from receiver to receiver. More iterations are required for a greater number of scattered reflections in the wave field, while fewer iterations are necessary in shadow zones of the acoustic field (e. g. see Figure 6, behind the dome). The influence of reflections is very evident for the greater number of screens in Case 2 and Case 3 (see Figures 7 and 8). As the excitation frequency increases (from 2.0 Hz to 100.0 Hz) the number of iterations required also increases.

The performance of the iterative coupling formulation relative to the full coupling formulation is enhanced when the number of screens present in the simulation increases. It can be seen that the difference in CPU times between the two formulations is greater for Case 3 than for Case 2 or Case 1. This shows that in terms of CPU, the iterative coupling is competitive when modeling a large number of inclusions.

An additional simulation has been performed for the same geometry as in Case 3, but changing the value of Δf from $\Delta f = 2$Hz to a lower value, $\Delta f = 0.5$Hz, and to a higher, $\Delta f = 4$Hz value. Figure 9 shows the results obtained when the excitation frequency is 100.0 Hz. Comparing Figure 9 with Figure 8 it is clear that when the Δf is reduced (the damping decreases) the CPU time and the number of iterations increase. On the other hand, the increase of Δf (from $\Delta f = 2$Hz to $\Delta f = 4$Hz) leads to a fall in the CPU time and the number of iterations required.

5 Time responses using the proposed iterative coupling formulation

The Case 3 scenario has been used to compute time responses (see Figure 5). The computations are performed in the frequency domain, for frequencies ranging from

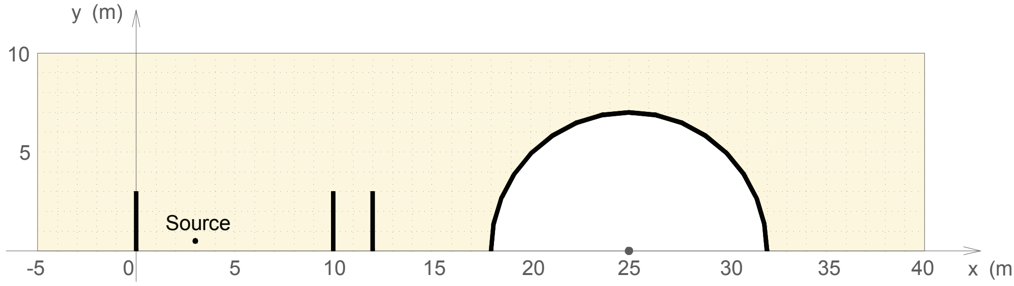

Figure 5: Geometry of the problem

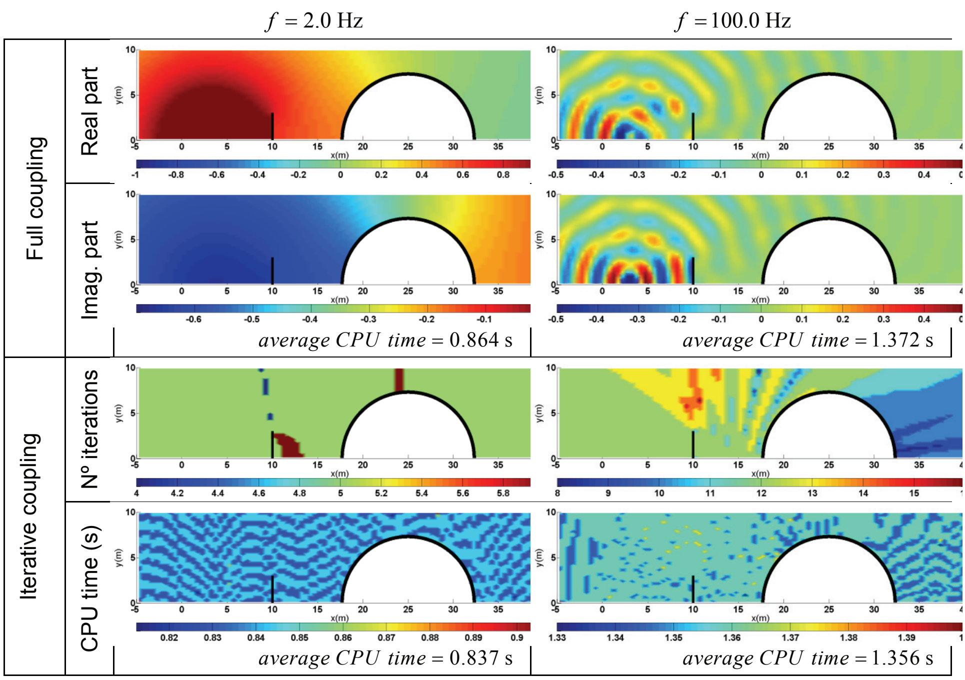

Figure 6: Acoustic problem – one barrier

2 Hz to 1024 Hz, with a frequency increment of 2 Hz, which determines a total time window for the analysis of 0.5 s.

The pressure response is obtained over the two-dimensional grid of receivers described above.

Each acoustic barrier is modeled as a rigid screen using the TBEM. It has null

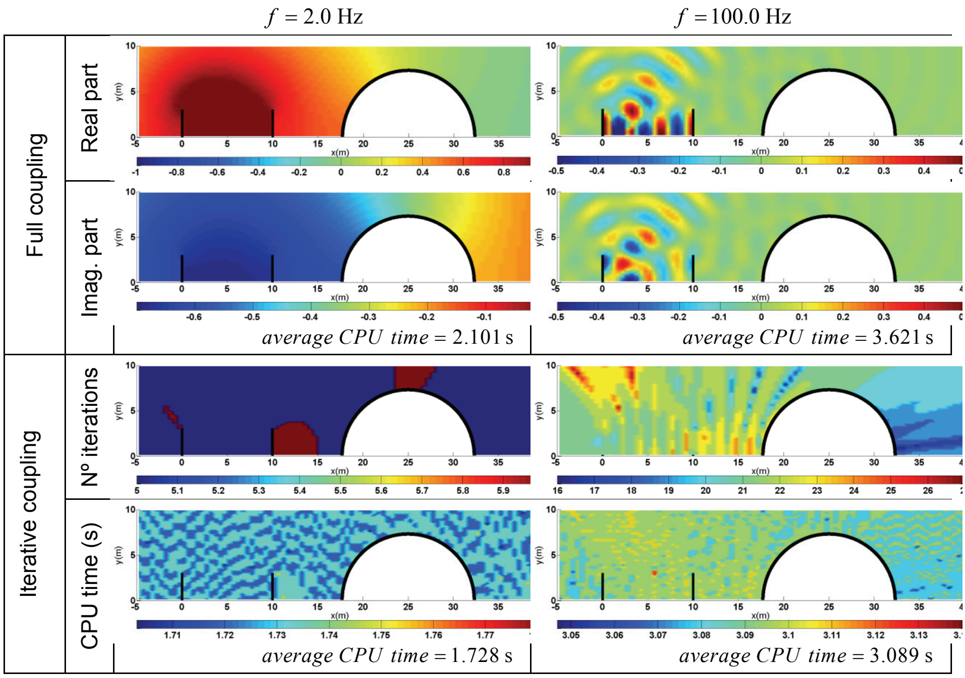

Figure 7: Acoustic problem – two barriers

thickness and is discretized using a number of boundary elements that changes from frequency to frequency. A ratio of 8 between the wavelength and the length of the boundary element was used. In any case a minimum number of 50 boundary elements was set.

The dome is assumed to be rigid and simulated by MFS, using virtual loads/collocation points that changed from frequency to frequency according to the ratio between the wavelength and the distance between collocation points, which was set at 8. A minimum of 200 virtual loads/collocation points were used. In the present example, the virtual loads are placed 0.7 m from its boundary. This distance was determined based on the calculation of errors at additional receivers placed along the boundary. The problem uses Green's functions appropriate for a half-space, assuming a rigid floor.

Time domain responses are obtained by applying an inverse Fourier transform to the frequency domain pressure wave field. The source is assumed to be a Ricker wavelet with a characteristic frequency of 300 Hz. Time domain responses are depicted in a set of graphs presented in Figures 10a) to 10f) where red represents

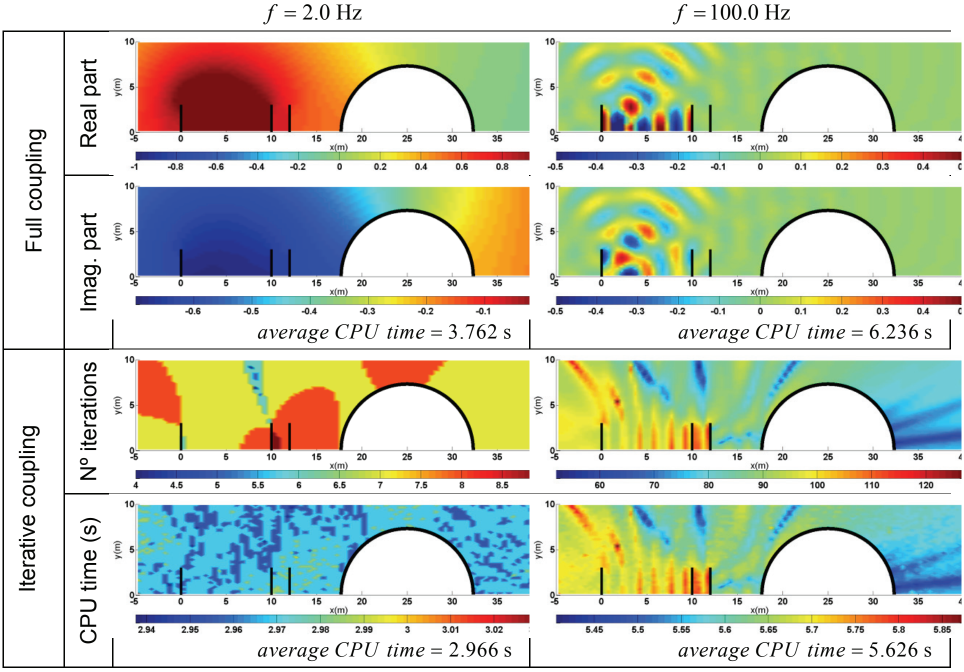

Figure 8: Acoustic problem – three barriers

the higher pressure amplitudes and blue the lower ones.

Figure 10a) shows the response at $t = 6.10$ ms when the incident pulse has already been reflected from the ground. At $t = 12.21$ ms (Figure 10b)) the incident and reflected pulses have reached the screen placed at y=0. 0 m, from which they are reflected. The wave diffraction at the top of the screen can also be seen. Then the diffracted pulse propagates towards the ground where it is reflected back (see Figure 10c), $t = 23.19$ ms). At this instant, the wave front propagating towards the dome has impacted the screen placed at y=10. 0 m, from where it is reflected back and diffracted at the top of the screen. Figure 10d) illustrates the pressure wave field at $t = 31.74$ ms where the pulses diffracted at the second screen have reached the screen placed at y=12.0, where they are also diffracted. Meanwhile the first diffracted pulse propagates forward and the second diffracted pulse propagates backward. At $t = 48.83$ ms (Figure 10e)) additional reflections and diffractions can be seen at the screens and the wave front impinged the dome's surface, from where it is reflected. As the time passes, additional reflections occur at the dome's surface and waves are trapped between screens due to multireflections (see Figure 10f)) $t = 65.92$ ms).

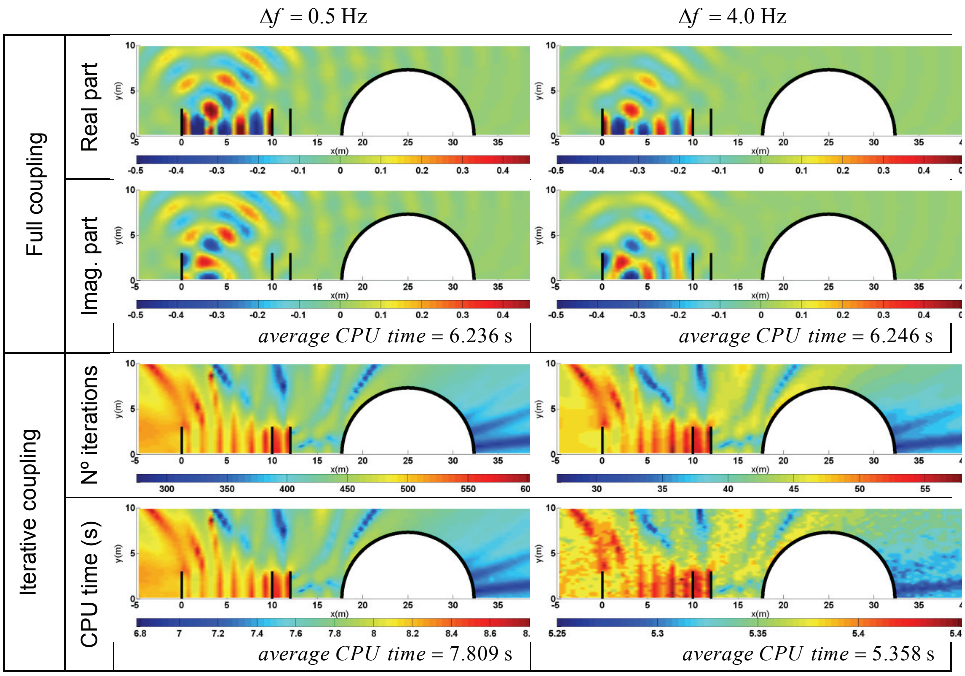

Figure 9: Acoustic problem – three barriers $f = 100.0$ Hz

6 Conclusions

An iterative coupling between the formulation based on the normal derivative of the integral equation (TBEM) and the method of fundamental solutions (MFS) has been proposed for the transient analysis of acoustic wave propagation problems in the presence of multi-inclusions.

At each step, only one inclusion is solved at a time, which leads to small system of equations and thus to reduced matrix storage requirements. As the coefficient matrixes remain the same, the system of equations is only solved once during the first iteration. The proposed iterative coupling formulation has been compared with a full coupling formulation. For a particular frequency, the number of iterations and CPU time varies from receiver to receiver depending on the scattered reflections in the wavefield. The number of iterations and CPU time increase for high frequencies and for low frequency steps.

It is concluded that in terms of CPU time the iterative coupling is competitive when modeling a large number of inclusions, when compared with a full coupling formulation.

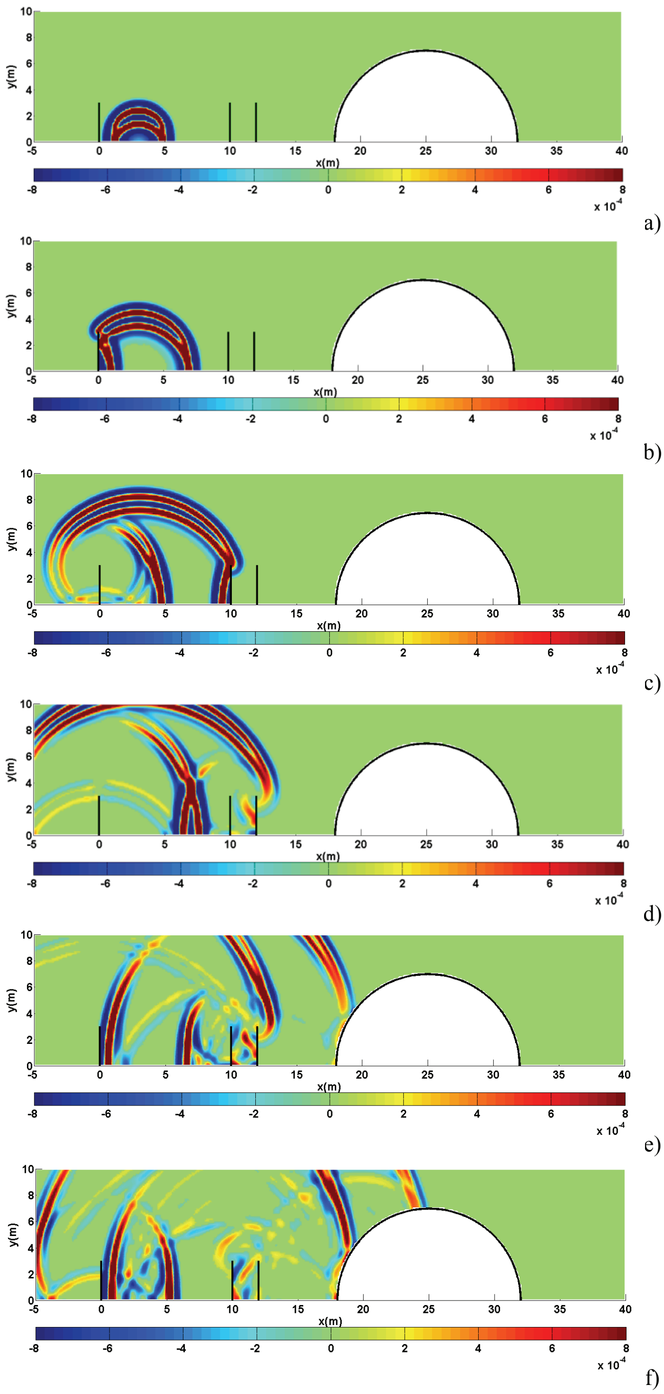

Figure 10: Pressure amplitude in time domain for Case 3 for a characteristic frequency of 300 Hz a) $t = 6.10$ ms; b) $t = 12.21$ ms; c) $t = 23.19$ ms; d) $t = 31.74$ ms; e) $t = 48.83$ ms; f) $t = 65.92$ ms.

The capabilities of the proposed technique have been illustrated by computing a numerical example that simulates the pressure wave propagation in the vicinity of a circular dome and three straight screens.

References

Acosta, S.; Villamizar, V. (2010) Coupling of Dirichlet-to-Neumann boundary condition and finite difference methods in curvilinear coordinates for multiple scattering. *J. Comput. Phys.*, vol. 229, pp. 5498–5517.

Aliaa, A.; Sadokb, H.; Soulia, M. (2012) CMRH method as iterative solver for boundary element acoustic systems. *Engineering Analysis with Boundary Elements*,vol. 36, no 3, pp. 346–350.

Alves C. J. S.; Leitão, V. M. A. (2006) Crack analysis using an enriched MFS domain decomposition technique. *Eng. Anal. Bound. Elem.*, vol. 30, pp. 160-166.

Antoine, X.; Chniti, C.; Ramdani, K. (2008) On the numerical approximation of high-frequency acoustic multiple scattering problems by circular cylinders. *J. Comput. Phys.*, vol. 227, pp. 1754–1771.

Benamou J. D.; Desprès B. (1997) A domain decomposition method for the Helmholtz equation and related optimal control problems. *Journal of Computational Physics*vol. 136, pp. 68–82.

Castro, I.; Tadeu, A. (2012) Coupling the BEM/TBEM and the MFS for the numerical simulation of elastic wave propagation. *Engineering Analysis with Boundary Elements*, vol. 36, pp. 169-180.

Defos du Rau, M.; Pessan, F.; Vigneras-Lefebvre; VPameix, J.P. (1996) Multiple scattering in heterogeneous media with spherical inclusions, *Computation in Electromagnetics*, 10-12 April 1996, Conference Publication No. 420, IEE.

Fairweather, G.; Karageorghis, A.; Martin, P.A. (2003) The method of fundamental solutions for scattering and radiation problems. *Eng. Anal. Bound. Elem.*, vol. 27, pp. 759-769.

Farhat C.; Macedo A.; Lesoinne M.; Roux F. X.; Magoules F.; de la Bourdonnaie A. (2000) Two-level domain decomposition methods with Lagrange multipliers for the fast iterative solution of acoustic scattering problems. *Computer Methods in Applied Mechanics and Engineering*,vol. 184, pp. 213–239.

Feng Y. T.; Owen D. R. J. (1996) Iterative solution of coupled FE/BE discretization for plate-foundation interaction problems. *Int J Numer Methods Eng.*, vol. 39, no.11, pp.1889–1901.

Gabrielli, P.; Mercier-Finidori, M. (2001) Acoustic scattering by two spheres: multiple scattering and symmetry considerations. *J. Sound Vibr.*,vol. 241, pp. 423-439.

Godinho, L.; Amado Mendes, P.; Tadeu, A.; Cadena-Isaza, A.; Smerzini, C.; Sánchez-Sesma, F. J.; Madec, R.; Komatitsch, D. (2009) Numerical simulation of ground rotations along 2D topographical profiles under the incidence of elastic plane waves. *Bull. Seism. Soc. Am.,* vol 99(2B), pp. 1147-1161.

Godinho, L.; Tadeu, A.; Simões, N. A. (2006) *Accuracy of the MFS and BEM on the analysis of acoustic wave propagation and heat conduction problems*. Sladek Jan and Sladek Vladimir, editors. Advances in Meshless Methods: Tech Science Press.

Greenberg, M. D. (1971) *Application of Green's Functions in Science and Engineering*. Prentice Hall, Englewood Cliffs.

Grote, M.; Kirsch, C. (2004) Dirichlet-to-Neumann boundary conditions for multiple scattering problems. *J. Comput. Phys.,* vol. 201, pp. 630–650.

Hampel, S.; Langer, S.; Cisilino, A. P. (2008) Coupling boundary elements to a raytracing procedure *International Journal for Numerical Methods in Engineering*, vol. 73,pp. 427–445.

He Z. C.; Liu G. R.; Zhong Z. H.; Zhang G. Y.; Cheng A. G. (2011) A coupled ES-FEM/BEM method for fluid structure interaction problems. *Eng. Anal. Bound. Elem.*,vol. 35, pp. 140-147.

Huang, Y.; Lu, Y. (2006) Scattering from periodic arrays of cylinders by Dirichlet-to-Neumann maps. *J. Lightwave Technol.* vol. 24, pp. 3448–3453.

Jawson, M. A.; Symm, G. T. (1977) *Integral Equation Methods in Potential theory and Elastostatics*. Academic, Press, London.

Kausel E.; Roesset J. M. (1992) Frequency domain analysis of undamped systems. *J Eng Mech, ASCE*, vol. 118,no. 4, pp. 721–734.

Lie S.T.; Yu, G.; Zhao, Z. (2001) Coupling of BEM/FEM for time domain structural-acoustic interaction problems. *CMES: Computer Modeling in Engineering & Sciences*, vol. 2, no. 2, pp. 171-182.

Lin C-C.; Lawton E. C.; Caliendo J. A.; Anderson L. R. (1996) An iterative finite element-boundary element algorithm. *Comput Struct.,*vol. 39, no 5, pp. 899–909.

Marburg, S.; Schneider, S. (2003) Performance of iterative solvers for acoustic problems. Part I. Solvers and effect of diagonal preconditioning. *Engineering Analysis with Boundary Elements*,vol. 27, no 7, pp. 727–750.

Rüberg, T.; Schanz, M. (2008) Coupling finite and boundary element methods for static and dynamic elastic problems with non-conforming interfaces. *Comput. Methods Appl. Mech. Engrg.*, vol. 198, pp. 449–458.

Soares, Jr. D.; Mansur, W. J. (2005) An Efficient Time-Domain BEM/FEM Coupling for Acoustic-Elastodynamic Interaction Problems. *CMES: Computer Modeling in Engineering & Sciences*, vol. 8, no. 2, pp. 153-164.

Soares D. Jr.; von Estorff O.; Mansur W. J. (2004) Iterative coupling of BEM and FEM for nonlinear dynamic analyses. *Comput Mech*, vol. 34, pp.67–73.

Soares Jr., D.;Godinho, L.; Pereira,A.; Dors, C. (2012) Frequency domain analysis of acoustic wave propagation in heterogeneous media considering iterative coupling procedures between the method of fundamental solutions and Kansa's method, *International Journal for Numerical Methods in Engineering* vol. 89, pp. 914–938.

Soares Jr. D; Mansur W.J. (2006) Dynamic analysis of fluid-soil-structure interaction problems by the boundary element method. *Journal of Computational Physics*, 219:498–512.

Soares Jr. D. (2009) Acoustic modelling by BEM-FEM coupling procedures taking into account explicit and implicit multi-domain decomposition techniques. *International Journal for Numerical Methods in Engineering*, vol. 78, pp. 1076–1093.

Tadeu A.; Santos P.; Kausel E. (1999) Closed-form integration of singular terms for constant, linear and quadratic boundary elements. Part I. SH wave propagation *Eng. Anal. Bound. Elmts*,vol. 23, no. 8,pp. 671–681.

Tadeu, A.; António, J.; Godinho, L. (2009) Defining an Accurate MFS Solution for 2.5D Acoustic and Elastic Wave Propagation. *Eng. Anal. Bound. Elem.*, vol. 33, pp. 1383-1385.

Tadeu A.; António J.; Castro I. (2010a) Coupling the BEM/TBEM and the MFS for the numerical simulation of acoustic wave propagation. *Eng. Anal. Bound. Elem.* vol. 34, pp. 405-416.

Tadeu, A.; Simões, N.; Simoes, I. (2010b) Coupling BEM/TBEM and MFS for the simulation of transient conduction heat transfer. *International Journal for numerical Methods in Engineering*, vol. 84, pp. 179-213.

Tadeu, A.; Castro, I. (2011) Coupling the BEM/TBEM and the MFS for the numerical simulation of wave propagation in heterogeneous fluid-solid media. *Mathematical Problems in Engineering*Article ID 159389, 26 p. (doi:10.1155/2011/159389).

Valente, F. P.; Pina, H. L. (2001) Iterative techniques for 3-D boundary element method systems of equations. *Engineering Analysis with Boundary Elements*,vol. 25, no. 6, pp. 423–429

von Estorff, O.; Hagen, C. (2006) Iterative coupling of FEM and BEM in 3D transient elastodynamics *Engineering Analysis with Boundary Elements*, vol. 30, pp. 611–622.

Warszawski, A.; Soares, D. Jr.; Mansur, W. J. (2008) A FEM–BEM coupling procedure to model the propagation of interacting acoustic–acoustic/acoustic–elastic waves through axisymmetric media. *Comput. Methods Appl. Mech. Eng.*, vol.197, pp. 3828-3835.

Ylä-Oijala, P.; Järvenpää, S. (2006) Iterative solution of high-order boundary element method for acoustic impedance boundary value problems. *Journal of Sound and Vibration*, vol. 291, no. 3-5, pp. 824-843.

Zheng Q.; Wang, J.; Li, J-ya (2011) The coupling method with the naturalboundary reduction on an ellipse for exterior anisotropic problems *CMES: Computer Modeling in Engineering & Sciences*, vol. 72, no. 2, pp. 103-114.